

Magnetic Structures and Properties of $Mn_{1-t}Co_tAs$

KARI SELTE,^a ARNE KJEKSHUS,^a GUNNAR VALDE^a and ARNE F. ANDRESEN^b

^a Kjemisk Institutt, Universitetet i Oslo, Blindern, Oslo 3, Norway and ^b Institutt for Atomenergi, Kjeller, Norway

The pseudo-binary MnAs–CoAs system has been investigated by X-ray and neutron diffraction and magnetic susceptibility measurements. $Mn_{1-t}Co_tAs$ exhibits slightly temperature dependent regions of limited solid solubility ($0 \leq t \leq 0.20 \pm 0.03$, $0.50 \pm 0.05 \leq t \leq 1$ below 350 °C). At lower temperatures the crystal structure is of the MnP type, except for a very small range near the composition MnAs, where the NiAs type structure prevails. At higher temperatures the NiAs type structure predominates. In both structure types the substituted atoms are randomly distributed over the metal sub-lattices.

The temperature characteristics of the magnetic susceptibility show a consistent trend in their changes with t above room temperature, the Curie-Weiss Law being fulfilled in the region of the high temperature NiAs type structure.

The low temperature NiAs type phase exhibits ferromagnetism. A double, a -axis helimagnetic mode is found below 196–152 K for Mn-rich $Mn_{1-t}Co_tAs$ samples ($0.05 \leq t \leq 0.15$) with MnP type structure. The spiral parameters depend both on composition and temperature.

Earlier communications consider the interesting magnetic properties of $V_{1-t}Mn_tAs$,¹ $Cr_{1-t}Mn_tAs$,^{2,3} and $Mn_{1-t}Fe_tAs$,⁴ all of which take the MnP type structure with random distribution of the two kinds of metal atoms over the metal sub-lattice. Since CoAs⁵ (like VAs,⁶ CrAs,⁷ MnAs (40–120 °C),⁸ and FeAs⁹) takes this structure type, “symmetry considerations” suggest that it may be rewarding to explore the magnetic properties of $Mn_{1-t}Co_tAs$.

EXPERIMENTAL

The binary compounds MnAs and CoAs were prepared by heating weighed quantities

of the elements [(99.9+ % Mn (The British Drug Houses; crushed powder from commercial, electrolytic grade material), 99.99+ % Co (Johnson, Matthey & Co.; turnings from rods), and 99.9999 % As (Koch-Light Laboratories)] in evacuated, sealed quartz tubes as described in Refs. 4 and 5. The binary arsenides were mixed in proportions according to the desired ternary compositions and subjected to a series of annealings at 850 or 1000 °C, interrupted by intermediate crushings. The samples were then cooled to 600 °C over 2 d and finally quenched in ice water.

The applied experimental techniques (X-ray and neutron diffraction and magnetic susceptibility measurements) have been described earlier.¹⁰

RESULTS

(i) *Homogeneity ranges and atomic arrangements.* An isothermal cross-section of the pseudo-binary MnAs–CoAs system at room temperature (as derived from samples quenched from 600 °C) shows that this system exhibits a two-phase miscibility gap for $0.20 \pm 0.03 < t < 0.50 \pm 0.05$ of the formula $Mn_{1-t}Co_tAs$. The limits of the solid solubility ranges have been determined from the variations in the unit cell dimensions with t (Fig. 1), and further confirmed by application of the disappearing phase principle to the X-ray powder data. Samples with atomic (Mn + Co)/As ratios different from 1.00 have not been examined in this study. As evident from Fig. 1 the NiAs and MnP type structures are alternating as the stable atomic arrangement at room temperature in the Mn-rich region of $Mn_{1-t}Co_tAs$. Thus, the NiAs type structure prevails for $0.00 \leq t < \sim 0.01$ and $0.10 \pm 0.01 \leq t \leq 0.20 \pm 0.03$, whereas the MnP type governs the rest of the single phase fields stated above.

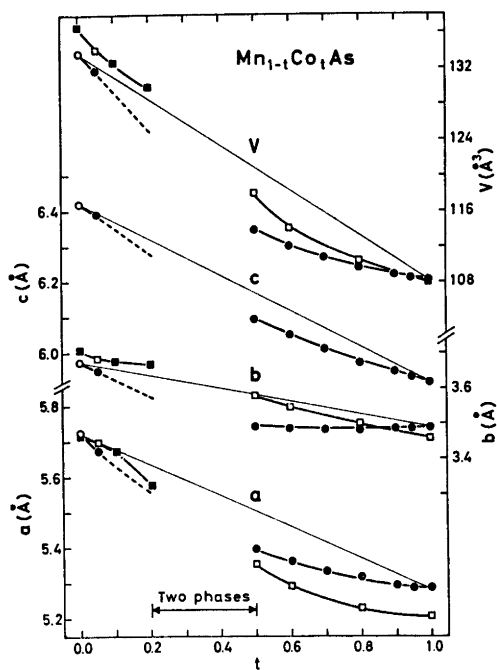


Fig. 1. Room temperature unit cell dimensions of $Mn_{1-t}Co_tAs$ as functions of t for samples quenched from 600 °C (filled symbols). Open symbols represent values derived by extrapolation from high temperature data. Circles and squares refer to MnP and NiAs type structures, respectively.

The crystallographic and magnetic phase relationships in the MnAs–CoAs system are illustrated in Fig. 2, where data for the system VAs–MnAs¹ are included for the purpose of comparison. Apart from a slight broadening of the two-phase field, the most prominent feature of the high temperature portion of the phase diagram is the complete predominance of the NiAs type structure. Since the NiAs type atomic arrangement occurs as both low and high temperature forms in MnAs, the designations I and II, respectively, introduced in Ref. 1, are conveniently adopted here. The second or higher order $MnP \rightleftharpoons NiAs(II)$ type transition in $Mn_{1-t}Co_tAs$ is detected by low and high temperature neutron and X-ray (Fig. 3) diffraction methods, as well as by magnetic susceptibility measurements (see ii).

X-Ray and neutron diffraction data show that the substituted atoms are randomly distributed over the metal sub-lattices in both the MnP and NiAs type atomic arrangements at all temperatures. The unit cell dimensions and positional parameters for the samples studied by neutron diffraction are listed in Table 1.

(ii) *Magnetic susceptibility.* The temperature characteristics of the reciprocal magnetic susceptibility show a consistent trend in their changes with the composition parameter t

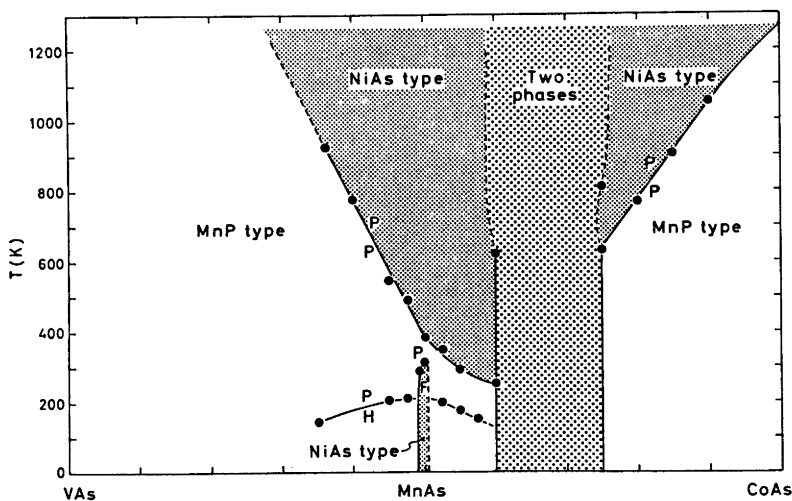


Fig. 2. Composite phase diagrams for the pseudo-binary VAs–MnAs¹ and MnAs–CoAs systems. Boundaries indicated by broken lines are uncertain. Magnetic state is indicated by: P para., F ferro., H helical.

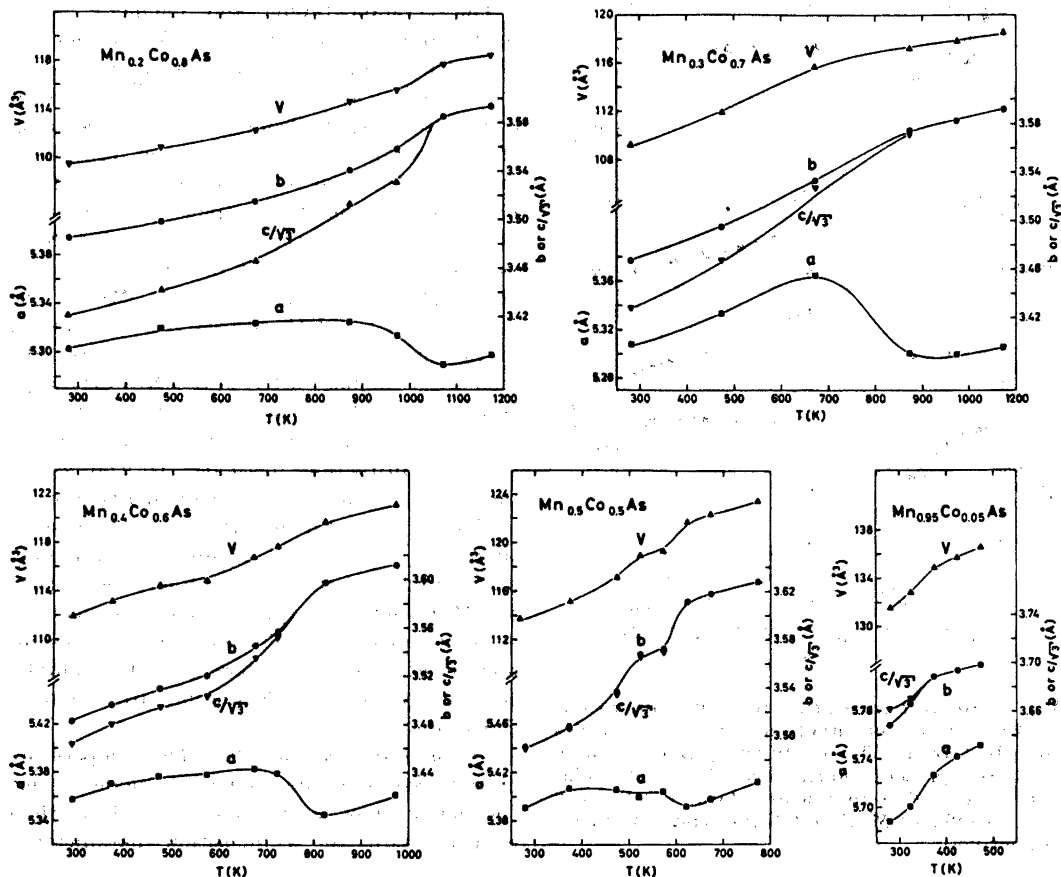


Fig. 3. Unit cell dimensions of selected $Mn_{1-x}Co_xAs$ samples versus temperature. Average relative expansion coefficients $\alpha_a = [(a_T - a_{T'})/a_{300}(T - T')]$, α_b , α_c multiplied by 10^6 K are 68, 125, 74; 9, 90, 90; 14, 41, 42; 35, 56, 80; and 4, 26, 41 for $Mn_{0.95}Co_{0.05}As$ (280–350 K), $Mn_{0.80}Co_{0.80}As$ (300–500 K), $Mn_{0.60}Co_{0.60}As$ (300–600 K), $Mn_{0.30}Co_{0.70}As$ (300–600 K), and $Mn_{0.10}Co_{0.90}As$ (300–800 K), respectively.

Table 1. Unit cell dimensions and positional parameters with standard deviations for some $Mn_{1-x}Co_xAs$ samples as derived by least squares profile refinements of neutron diffraction data. (Space group $Pnma$; positions 4(c); overall profile reliability factors ranging between 0.039 and 0.061.)

| x | T (K) | a (Å) | b (Å) | c (Å) | x_T | z_T | x_X | z_X |
|------|------------------|------------|------------|------------|-----------|----------|----------|----------|
| 0.05 | 4.2 | 5.5662(7) | 3.5151(4) | 6.1825(11) | -0.005(3) | 0.222(4) | 0.189(2) | 0.587(1) |
| | 79 | 5.5755(9) | 3.5254(6) | 6.1964(14) | 0.006(3) | 0.214(4) | 0.198(1) | 0.584(2) |
| | 293 | 5.6875(18) | 3.6541(19) | 6.3494(25) | 0.009(2) | 0.226(3) | 0.220(1) | 0.590(3) |
| 0.10 | 4.2 | 5.5539(8) | 3.5252(5) | 6.1843(12) | 0.008(8) | 0.215(3) | 0.191(2) | 0.584(2) |
| | 79 | 5.5591(8) | 3.5322(5) | 6.1928(12) | 0.013(3) | 0.214(3) | 0.197(1) | 0.587(2) |
| | 293 ^a | 5.6702(11) | 3.6764(5) | [6.3679] | [0] | [1/4] | [1/4] | [7/12] |
| 0.15 | 5 | 5.5429(7) | 3.5359(5) | 6.1843(12) | 0.014(2) | 0.218(2) | 0.194(1) | 0.583(2) |
| | 79 | 5.5461(8) | 3.5417(6) | 6.1969(14) | 0.013(3) | 0.216(3) | 0.198(1) | 0.584(2) |
| | 293 ^a | 5.6241(11) | 3.6722(5) | [6.3603] | [0] | [1/4] | [1/4] | [7/12] |

^a NiAs type structure.

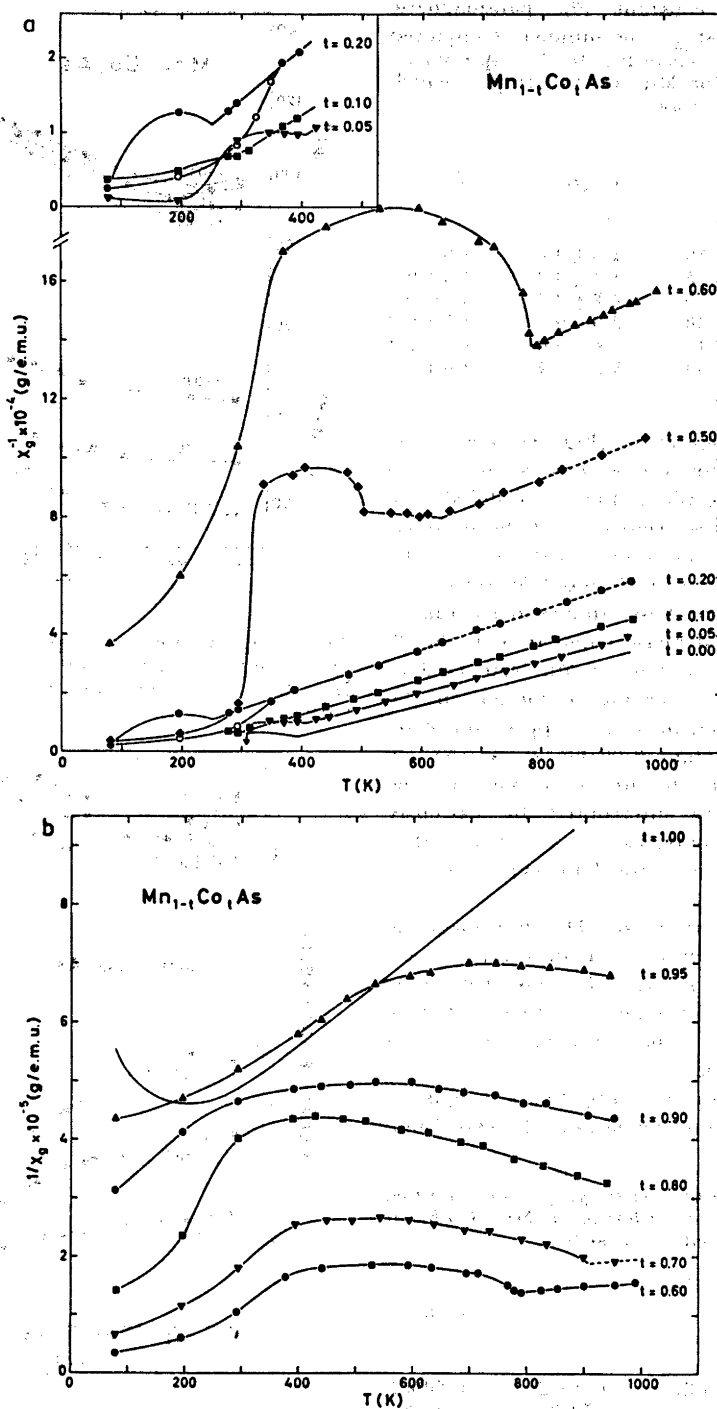


Fig. 4. Reciprocal magnetic susceptibility for typical $Mn_{1-t}Co_tAs$ samples: (a) $0 \leq t \leq 0.60$ and (b) $0.60 \leq t \leq 1$.

Table 2. Curie constant (θ), paramagnetic moment ($\mu_P = \sqrt{8C_M}$), and number of unpaired electrons ($n = 2S_T$; according to the "spin only" approximation) for $Mn_{1-t}Co_tAs$ samples which fulfil Curie-Weiss Law.

| t | θ (K) | μ_P (μ_B) | $2S_T$ |
|------|---------------|---------------------|---------------|
| 0.00 | 270 ± 10 | 4.5 ± 0.3 | 3.6 ± 0.2 |
| 0.05 | 235 ± 15 | 4.3 ± 0.3 | 3.5 ± 0.2 |
| 0.10 | 200 ± 15 | 4.2 ± 0.3 | 3.3 ± 0.2 |
| 0.20 | 100 ± 20 | 3.9 ± 0.3 | 3.1 ± 0.2 |
| 0.50 | -320 ± 40 | 3.6 ± 0.4 | 2.7 ± 0.3 |
| 0.60 | -750 ± 50 | 3.5 ± 0.4 | 2.6 ± 0.3 |

above room temperature (Fig. 4). The linear $\chi^{-1}(T)$ portions for single phase samples with $0 \leq t \leq 0.70$ (Curie-Weiss Law is fulfilled) are associated with the occurrence of the NiAs(II) type structure. The broken sections on the characteristics for $t=0.20$ and 0.50 refer to a two-phase status of these samples in accordance with the indicated phase boundaries in Fig. 2. With decreasing content of Mn from $t=0$ to $t=0.60$ there is a gradual reduction in the paramagnetic moment, and an appreciable drop in the Curie constant θ (Table 2). At the low temperature side the linear sections of the $\chi^{-1}(T)$ curves are interrupted by variously shaped, curved portions, thus evincing that the transformation to the MnP type structure has occurred.

(iii) *Magnetic structures.* The ferromagnetic mode of MnAs,¹¹ with moments arranged perpendicular to the hexagonal c axis of its NiAs type atomic arrangement, extends slightly ($t < \sim 0.01$) into the ternary region of $Mn_{1-t}Co_tAs$ (cf. Fig. 2).

At low temperatures, $Mn_{1-t}Co_tAs$ samples in the composition range $0.05 \leq t \leq 0.15$ were found

Table 3. Parameters specifying the double, a -axis helimagnetic ordering in $Mn_{1-t}Co_tAs$ at 79 K (β is assumed to be 90°).

| t | 0.05 | 0.10 | 0.15 |
|---------------------|----------|----------|----------|
| $\tau/2\pi a^*$ | 0.166(2) | 0.184(2) | 0.209(2) |
| μ_T (μ_B) | 1.80(3) | 1.72(3) | 1.66(3) |
| ϕ ($^\circ$) | 95(3) | 100(3) | 104(3) |
| T_N (K) | 196(1) | 174(1) | 152(1) |

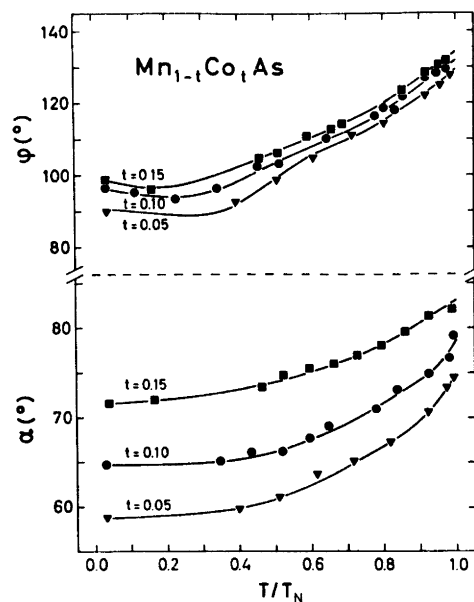


Fig. 5. Spiral turn angle per a -length (α) and phase angle (ϕ) for $t=0.05, 0.10$, and 0.15 of $Mn_{1-t}Co_tAs$ as functions of reduced temperature.

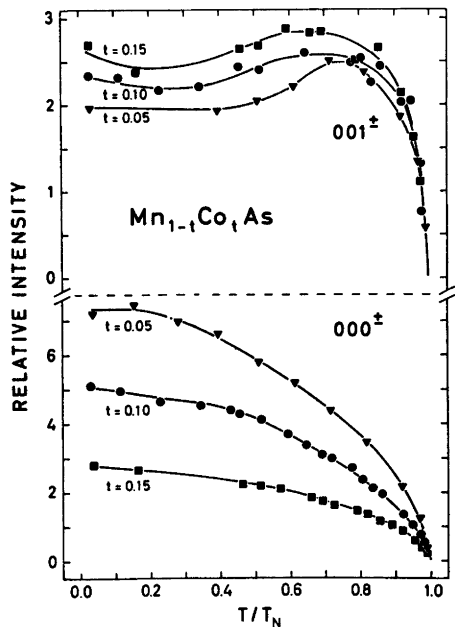


Fig. 6. Relative, integrated intensities of $000\pm$ and $001\pm$ versus reduced temperature for $t=0.05, 0.10$, and 0.15 of $Mn_{1-t}Co_tAs$.

to take the double, a -axis type helimagnetic mode earlier observed for $\text{V}_{1-t}\text{Mn}_t\text{As}$ ($\sim 0.60 \leq t \leq 0.95$)¹ and $\text{Mn}_{1-t}\text{Fe}_t\text{As}$ ($\sim 0.01 < t < \sim 0.12$).⁴ Parameters describing this helimagnetic arrangement, are magnetic moment per metal atom (μ_T), spiral propagation vector (τ), phase angle between independent spirals (ϕ), and angle between moment and spiral axis (β), numerical values being given in Table 3 together with the Néel temperatures (T_N) for samples with $t=0.05$, 0.10, and 0.15. As seen from Fig. 2 and Table 3, T_N and μ_T decrease with increasing t . These results are in conformity with those for $\text{V}_{1-t}\text{Mn}_t\text{As}$ ($0.70 \leq t \leq 0.95$). All MnP type phases with the double, a -axis type helimagnetic mode studied^{1,4} so far have shown substantial variation of the propagation vector and phase angle with composition and temperature. As seen from Fig. 5 and Table 3, the $\text{Mn}_{1-t}\text{Co}_t\text{As}$ phase ($0.05 \leq t \leq 0.15$) makes no exception in this respect. However, as opposed to the situation for $\text{V}_{1-t}\text{Mn}_t\text{As}$, where α decreases with increasing V-content, α increases with t in $\text{Mn}_{1-t}\text{Co}_t\text{As}$.

The (reduced) temperature dependence of the integrated intensity for the strongest satellites $000\pm$ and $001\pm$ of $\text{Mn}_{0.95}\text{Co}_{0.05}\text{As}$, $\text{Mn}_{0.90}\text{Co}_{0.10}\text{As}$, and $\text{Mn}_{0.85}\text{Co}_{0.15}\text{As}$ are shown in Fig. 6. Following the procedure outlined in Refs. 1 and 4 and utilizing a similar $\mu_T/\mu_{T,0K}$ versus T/T_N relationship to that postulated in Ref. 1, the calculated curves for ϕ versus T/T_N in Fig. 5 are obtained. This demonstrates an internal consistency between the various data.

DISCUSSION

Neglecting the magnetic aspects, the phase diagrams of the pseudo-binary systems $T\text{As}-T'\text{As}$ (T or T' : V, Cr, Mn, Fe, or Co) with MnP type structure fall into two categories, according to whether there is complete or limited solid solubility. Consultations of unit cell volumes and interatomic distances for the binary compounds⁵⁻⁹ show that the Hume-Rothery¹² 15% criterion is not governing the distinction between these categories. Since $\text{MnAs}-\text{FeAs}$ ⁴ and $\text{MnAs}-\text{CoAs}$ are the only systems which exhibit regions of limited solid solubility, the guiding principle appears to be that of incompatibility of electronic band structures (cf. Ref. 13). The implications are

accordingly that MnAs has an electronic band structure which differs from those of FeAs and CoAs.

A common feature of all MnAs- T As systems is a second (or higher) order crystallographic transition between MnP and NiAs type structures.^{1,3,4} Consistent with geometrical¹⁴ and group theoretical¹⁵ considerations, similar $\text{MnP} \rightleftharpoons \text{NiAs}$ type transitions are also found in a number of other binary and ternary phases,^{14,16-19} but the conversion is there found at much higher temperatures. In this connection it is interesting to note that MnAs-CoAs is the only combination which results in a lowering of the temperature for the $\text{MnP} \rightleftharpoons \text{NiAs}$ transition. Among the T As compounds CoAs also provides the only example of an MnP type phase with an axial ratio $c/b < \sqrt{3}$ ($c/b \equiv \sqrt{3}$ for the NiAs type atomic arrangement). $\text{Mn}_{0.5}\text{Co}_{0.5}\text{As}$ provides an interesting example, where c/b stays constant at 1.732 at all temperatures (Fig. 3), also in the region where the MnP type structure prevails.

The question of whether the double, helimagnetic ordering propagates in the a or c direction is also connected with the particular combination of the binary monoarsenides. The fact that a axis spirals only have been observed for Mn-rich $\text{Mn}_{1-t}\text{T}_t\text{As}$ samples ($T = \text{V, Fe, Co}$) has led us to reconsider the available information on MnAs more carefully. (Revaluation of the data presented by Kazama and Watanabe³ for $\text{Cr}_{1-t}\text{Mn}_t\text{As}$ ($0.7 \leq t \leq 0.9$) suggests very strongly that this phase also takes the double, a -axis type helimagnetic structure. Work is in progress to verify this suggestion.) The magnetic exchange interactions are the factors which rule the cooperative magnetic arrangements, but these key parameters are in turn governed by *inter alia* the interatomic distances in the chemical structure. It may therefore be significant to note that just MnAs has the largest difference between the nearest and next nearest $T-T$ distances among the MnP type T As compounds. Thus, bearing in mind that the $T-T$ distances along the a direction in the MnP type MnAs structure are appreciably shorter than those in the b,c planes, and that the orientation of the ferromagnetic moments is perpendicular to the corresponding (c) direction in the NiAs(I) modification of MnAs, the arrangement of the moments in

planes perpendicular to c appears to be a natural consequence. The tendency towards spiral formation seems to originate from the zig-zag arrangement of the T atoms in the two mutually perpendicular directions. This observation together with a more careful analysis of the details of the various cooperative arrangements adopted by MnP type phases may lead to a resolution of the relation between the magnitudes of the exchange interaction parameters and the helical modes.

Acknowledgements. The assistance of Ing. Stanislav Vratilav (I.A.E.A.-fellow from The Technical University of Prague, Czechoslovakia) and cand.mag. Per G. Peterzens in the neutron diffraction measurements and the financial support of The Norwegian Research Council for Science and the Humanities are greatly appreciated.

REFERENCES

1. Selte, K., Kjekshus, A., Valde, G. and Andresen, A. F. *Acta Chem. Scand. A* 30 (1976) 8.
2. Watanabe, H., Kazama, N., Yamaguchi, Y. and Ohashi, M. *J. Appl. Phys.* 40 (1969) 1128.
3. Kazama, N. and Watanabe, H. *J. Phys. Soc. Jpn.* 30 (1971) 1319.
4. Selte, K., Kjekshus, A. and Andresen, A. F. *Acta Chem. Scand. A* 28 (1974) 61.
5. Selte, K. and Kjekshus, A. *Acta Chem. Scand.* 25 (1971) 3277.
6. Selte, K., Kjekshus, A. and Andresen, A. F. *Acta Chem. Scand.* 26 (1972) 4057.
7. Selte, K., Kjekshus, A., Jamison, W. E., Andresen, A. F. and Engebretsen, J. E. *Acta Chem. Scand.* 25 (1971) 1703.
8. Wilson, R. H. and Kasper, J. S. *Acta Crystallogr.* 17 (1964) 95.
9. Selte, K. and Kjekshus, A. *Acta Chem. Scand.* 23 (1969) 2047.
10. Selte, K., Kjekshus, A. and Andresen, A. F. *Acta Chem. Scand.* 26 (1972) 3101.
11. Bacon, G. E. and Street, R. *Nature* 175 (1955) 518.
12. Hume-Rothery, W. *The Structure of Metals and Alloys*, Institute of Metals, London 1936.
13. Furuseth, S., Selte, K. and Kjekshus, A. *Acta Chem. Scand.* 21 (1967) 527.
14. Selte, K. and Kjekshus, A. *Acta Chem. Scand.* 27 (1973) 3195.
15. Franzen, H. F., Haas, C. and Jelinek, F. *Phys. Rev. B* 10 (1974) 1248.
16. Ido, H. *J. Phys. Soc. Jpn.* 25 (1968) 1543.
17. Selte, K., Hjersing, H., Kjekshus, A. and Andresen, A. F. *Acta Chem. Scand. A* 29 (1975) 312.
18. Franzen, H. F. and Wieggers, G. A. *J. Solid State Chem.* 13 (1975) 114.
19. Selte, K., Hjersing, H., Kjekshus, A., Andresen, A. F. and Fischer, P. *Acta Chem. Scand. A* 29 (1975) 695.

Received January 29, 1976.